ANTICANCER RESEARCH *39*: 3443-3451 (2019)
doi:10.21873/anticanres.13490

Oxidative DNA Damage and Apoptosis Induced by Aclarubicin, an Anthracycline: Role of Hydrogen Peroxide and Copper

HIDEKI MIZUTANI[1], YUKA HAYASHI[1], MIYABI HASHIMOTO[1], MASANORI IMAI[1], YOSHIMI ICHIMARU[1], YUKI KITAMURA[1], KENJI IKEMURA[1,2], DAISUKE MIYAZAWA[1], KINYA OHTA[1], YOSHIAKI IKEDA[1], TOHRU MAEDA[1], MASAE YOSHIKAWA[1], YUSUKE HIRAKU[3] and SHOSUKE KAWANISHI[4]

[1]*College of Pharmacy, Kinjo Gakuin University, Nagoya, Japan;*
[2]*Department of Pharmacy, Mie University Hospital, Tsu, Japan;*
[3]*Department of Environmental Health, University of Fukui School of Medical Sciences, Eiheiji, Japan;*
[4]*Faculty of Pharmaceutical Sciences, Suzuka University of Medical Science, Suzuka, Japan*

Abstract. *Background/Aim: This study aimed to investigate aclarubicin (ACR)-induced oxidative DNA damage and apoptosis. Materials and Methods: ACR-induced apoptosis was analyzed using HL-60 leukemia cells and HP100 cells, hydrogen peroxide (H_2O_2)-resistant cells derived from HL-60 cells. ACR-induced DNA damage was analyzed using plasmid DNA. Results: HL-60 cells were more sensitive to ACR than HP100 cells. In HP100 cells, DNA ladder formation and caspase-3/7 activity induced by ACR were suppressed or delayed in comparison to those in HL-60 cells. ACR-induced DNA damage occurred in the presence of Cu(II), and scavenger experiments showed that the reactive species causing DNA damage appeared to be generated from H_2O_2 and Cu(I). Moreover, we detected intracellular Cu(I) induced by ACR in HL-60 cells, using CopperGREEN™, a fluorescent probe for detection of Cu(I) ion specifically. Conclusion: ACR-induced DNA damage and apoptosis can be accounted for by the involvement of H_2O_2 and Cu(I).*

Anthracyclines comprise one of the most important drug classes in anticancer treatment (1). One anthracycline, aclarubicin (aclacinomycin A, ACR), with a trisaccharide chain, was discovered and characterized by Umezawa *et al.* in the 1970s (2). ACR has potent efficacy against solid as well as hematological malignancies, and shows the same growth inhibition of solid sarcoma-180 and Gardner 6C3HED/OG lymphosarcoma transplanted subcutaneously in mice as doxorubicin and daunorubicin (3). The cardiotoxicity of ACR is weaker than that of doxorubicin in hamsters (4). ACR is clinically approved in Japan for treatment of cancer of the stomach, lung, breast and ovary, as well as acute leukemia and malignant lymphoma; ACR is often used in place of daunorubicin or idarubicin to reduce cardiotoxicity in patients with acute myeloid leukemia and myelodysplastic syndrome (5-7).

It is believed that the main anticancer action of anthracyclines is apoptosis through DNA damage (1). ACR-induced DNA damage is caused by inhibition of topoisomerase I and II, and by DNA intercalation and the action of reactive oxygen species (ROS) (8-11). It has been reported that ACR induced DNA damage and apoptosis, one cause of which was ROS generation (12, 13). However, the mechanism of ACR-induced ROS generation has not well been elucidated. In this study, we investigated apoptosis induced by ACR using human leukemia cell lines, HL-60, and HP100, a hydrogen peroxide (H_2O_2)-resistant clone derived from HL-60 cell line (14, 15). The apoptotic mechanisms were analyzed by examining cell viability assay, DNA ladder assay and caspase-3/7 activity assay. We also examined ACR-induced DNA damage using plasmid DNA and $O_2^{\bullet-}$ production in the presence of Cu(II) in a cell-free system. In addition, we detected intracellular Cu(I) induced by ACR using a fluorescent probe to detect Cu(I) ion specifically in HL-60 cells.

Materials and Methods

Materials. Aclarubicin hydrochloride was purchased from FUJIFILM Wako Pure Chemical Co. (Osaka, Japan). Superoxide dismutase (SOD; 3,000 U/mg from bovine erythrocytes), catalase (45,000 U/mg from bovine liver) and cytochrome c (from equine heart) were purchased from Sigma-Aldrich Co. (St. Louis, MO, USA). Plasmid DNA (pBR322) and DNA gel loading dye (6×) were from Toyobo Co. (Osaka, Japan). Copper chloride ($CuCl_2 \bullet 2H_2O$)

Correspondence to: Hideki Mizutani, Ph.D., College of Pharmacy, Kinjo Gakuin University, Moriyama-ku, Nagoya 463-8521, Japan. Tel.: +81 527987458, Fax: +81 527980754, e-mail: mizu@kinjo-u.ac.jp

Key Words: Aclarubicin, DNA damage, apoptosis, ROS, hydrogen peroxide, copper.

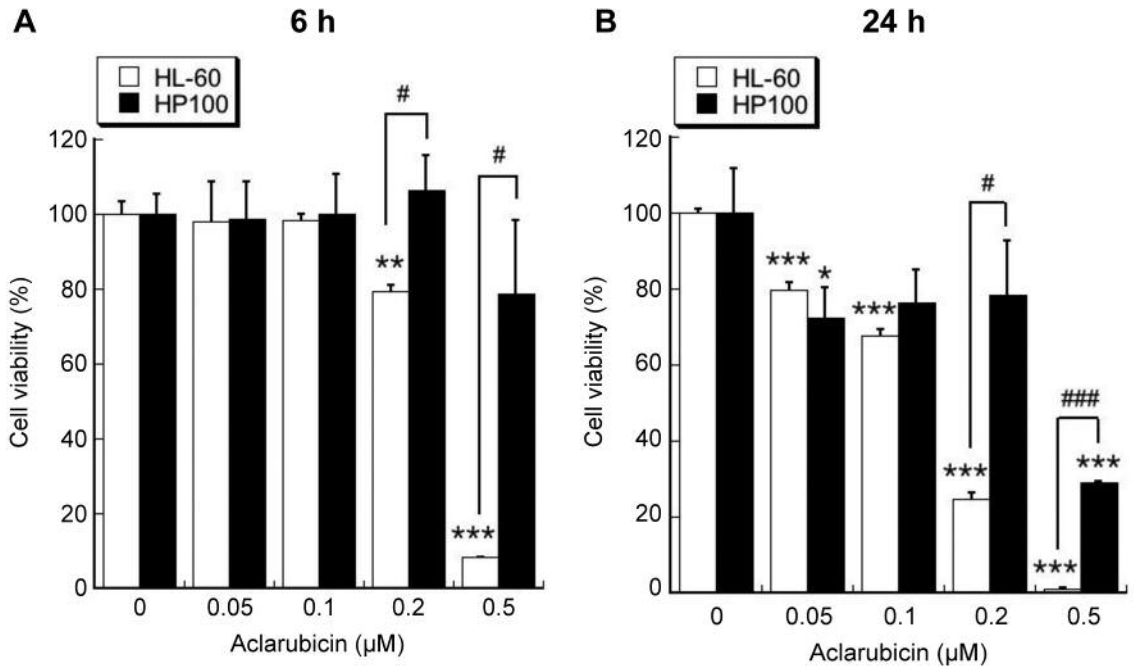

Figure 1. *Determination of cell viability in HL-60 and HP100 cells after treatment with aclarubicin (ACR) for 6 (A) and 24 h (B). After treatment, cell viability was determined by the luminescent assay kit. The data are presented as means±SD (n=3). Significantly different at: *p<0.05, **p<0.01 and ***p<0.001 vs. control by ANOVA followed by the Tukey's HSD test; #p<0.05 and ###p<0.001 by the Student's t-test.*

was from Nacalai Tesque Co. (Kyoto, Japan). Diethylenetriamine-*N,N,N',N'',N''*-penta-acetic acid (DTPA) and bathocuproine-disulfonic acid were from Dojindo Laboratories Co. (Kumamoto, Japan). Methional [3-(Methylthio)propionaldehyde] was from Tokyo Chemical Industry Co. (Tokyo, Japan). CopperGREEN™, a fluorescent probe used to detect Cu(I) ions, was from Goryo Chemical Inc. (Sapporo, Japan). All other chemicals used were of the highest purity commercially available.

Cell culture and treatment with ACR. Human leukemia HL-60 and HP100 cells were obtained from Riken BioResource Research Center (Tsukuba, Japan). HP100 cells have approximately 340-fold higher resistance to H_2O_2 (14) and 18 times higher catalase activity (15) than HL-60 cells. By use of HP100 cells, effects of intracellular catalase can be evaluated (16). HL-60 and HP100 cells were grown in RPMI 1640 (FUJIFILM Wako Pure Chemical Co.) supplemented with 6% fetal bovine serum (Biowest Co., Nuaillé, France) at 37˚C under 5% CO_2 in a humidified atmosphere. The cells (0.5×10^6 or 1×10^6 cells/ml) were then treated with 0.05, 0.1, 0.2 and 0.5 μM of ACR.

Determination of cell viability treated by ACR in HL-60 and HP100 cells. A luminescent assay kit quantitating the ATP present (CellTiter-Glo® Assay, Promega, Fitchburg, WI, USA) was used for determining the number of viable cells in culture. A total of 5.0×10^4 cells were seeded into each well of 96-well white cell culture plates (Thermo Fisher Scientific, Waltham, MA, USA). After ACR (0.05, 0.1, 0.2 and 0.5 μM) treatment for 6 h or 24 h, the cell viability was analyzed according to the manufacturer's explanatory notes.

Detection of ACR-induced apoptosis of HL-60 and HP100 cells. For analyses of DNA ladder formation in treated cells by ACR, cells were washed twice with phosphate-buffered saline (PBS). The fragmented DNA was extracted from HL-60 and HP100 cells (2×10^6 cells) according to previous reports (17, 18). DNA ladder formation was analyzed by conventional electrophoresis.

Analysis of caspase-3/7 activity in HL-60 and HP100 cells. A total of 5.0×10^4 cells were seeded into each well of 96-well black cell culture plates (Thermo Fisher Scientific). After ACR treatment (0.05, 0.1, 0.2 and 0.5 μM) for 6 h, caspase-3/7 activity was analyzed use of a caspase-3/7 activity fluorescent assay kit (Apo-ONE® Homogeneous Caspase-3/7 Assay; Promega, Fitchburg, WI, USA) according to the manufacturer's explanatory notes.

Analysis of ACR-induced DNA damage in the presence of Cu(II) in a cell-free system. The standard reaction solution in a 1.5 ml Eppendorf Tubes® 3810X (Eppendorf AG, Hamburg, Germany) contained ACR, 20 μM $CuCl_2$ and pBR322 plasmid DNA (0.2 μg/tube) in 50 μl of 10 mM sodium phosphate buffer (pH 7.8) containing 5 μM DTPA, a chelator, for removal of trace amounts of contaminating metals. After incubation at 37˚C for 60 min, DNA gel loading dye was added to the reaction solution and the reacted DNA was electrophoresed on a 0.7% agarose gel containing ethidium bromide. The obtained DNA gels were analyzed using a UV transilluminator (19, 20).

Analysis of ACR-induced DNA damage in the presence of metals in a cell-free system. The reaction solution placed in a 1.5 ml Eppendorf Tubes® 3810X contained 20 μM ACR, 20 μM metals

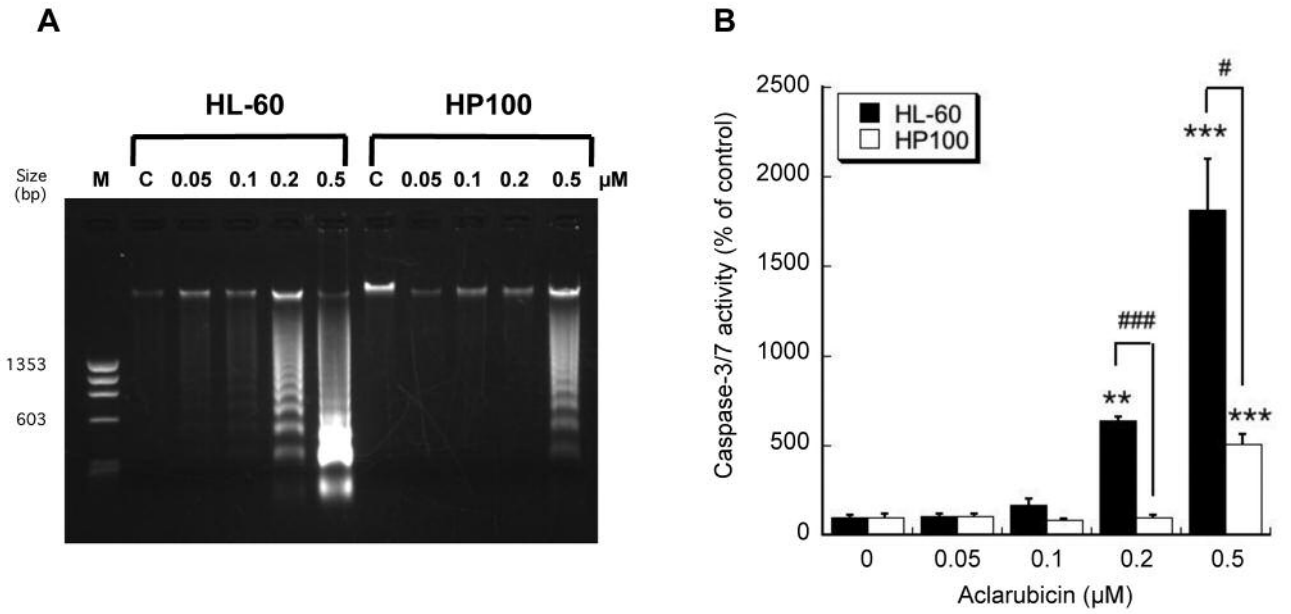

Figure 2. *Detection of aclarubicin (ACR)-induced apoptosis of HL-60 and HP100 cells. A: DNA ladder formation in HL-60 and HP100 cells after treatment with ACR for 6 h. The DNA was extracted from cell lysate and analyzed by conventional electrophoresis. Marker line: Size marker DNA (ΦX174/Hae III digest). B: Caspase-3/7 activation in HL-60 and HP100 cells treated with ACR for 6 h. After ACR treatment, caspase-3/7 activity was determined by caspase-3/7 activity assay kit. The data are presented as means±SD (n=3). Significantly different at: **p<0.01 and ***p<0.001 vs. control by ANOVA followed by the Tukey's HSD test; #p<0.05 and ###p<0.001 by the Student's t-test.*

($CuCl_2$, $FeCl_3$, $FeSO_4(NH_4)_2SO_4$, $ZnSO_4$, $NiSO_4$, $MgCl_2$, $CoCl_2$ or $MnCl_2$) and pBR322 plasmid DNA (0.2 μg/tube) in 50 μl of 10 mM sodium phosphate buffer (pH 7.8) containing 5 μM DTPA. After incubation at 37˚C for 60 min, the DNA gel loading dye was added to the reaction solution and the reacted DNA was electrophoresed on a 0.7% agarose gel containing ethidium bromide. The obtained DNA gels were analyzed by using a UV transilluminator (20).

Analysis of effects of ROS scavengers and bathocuproine on ACR-induced DNA damage in the presence of Cu(II) in a cell-free system. The reaction solution placed in a 1.5 ml Eppendorf Tubes® 3810X contained 20 μM ACR, 20 μM $CuCl_2$, pBR322 plasmid DNA (0.2 μg/tube) in 50 μl of 10 mM sodium phosphate buffer (pH 7.8) containing 5 μM DTPA with ROS scavengers and 50 μM bathocuproine, as a Cu(I)-chelating agent. ROS scavengers were 1.7 M (10%) ethanol, 0.1 M mannitol, 0.1 M sodium formate, 0.7 M (10%) dimethyl sulfoxide (DMSO), 50 or 100 units of SOD, 50 or 100 units of catalase, and 0.1 M methional. After incubation at 37˚C for 60 min, the DNA gel loading dye was added to the reaction solution and the reacted DNA was electrophoresed on a 0.7% agarose gel stained with ethidium bromide. The obtained DNA gels were analyzed by using a UV transilluminator (20).

Detection of $O_2^{\bullet-}$ derived from ACR in the presence of Cu(II) in a cell-free system. To detect $O_2^{\bullet-}$ generation from ACR, 100 μM cytochrome *c* was added to a reaction solution containing 20 μM ACR and 20 μM Cu(II) in 1 ml of 10 mM sodium phosphate buffer (pH 7.8) with 2.5 μM DTPA. The reduction of ferricytochrome c produces ferrocytochrome *c* that has an absorption maximum at 550 nm; absorption was measured at 37˚C with a UV-visible spectrophotometer (UV-2600; Shimadzu, Kyoto, Japan). The actual amount of reduced cytochrome *c* was calculated by subtracting absorbance with 100 U/ml SOD from that without SOD at 550 nm (ε=21.1×10^3 M^{-1} cm^{-1}) (20, 21).

Determination of intracellular Cu(I) induced by ACR in HL-60 cells. CopperGREEN™, a fluorescent probe for detection of Cu(I) ions, was used to determine intracellular Cu(I) in cultured cells (22). HL-60 cells (1×10^6 cells) were treated with ACR at 37˚C for 3 h in the presence of 5 μM CopperGREEN™. Cells were then washed twice with PBS. After resuspension in PBS, cells were analyzed using a fluorescence microscopy (EVOS® FLoid® Cell Imaging Station; Thermo Fisher Scientific). Obtained data were analyzed using Image J 1.43u (National Institute of Health, Bethesda, MD, USA).

Statistical analysis. All statistical analyses were performed using Kaleida Graph version 4.1.3 (Synergy Software, Reading, PA, USA). ANOVA followed by Tukey's HSD test was used to compare differences between the test groups and the control groups. Student's *t*-test was used to compare differences between the test groups. Values of $p<0.05$ were regarded as statistically significant.

Results

Cell viability in HL-60 and HP100 cells treated with ACR. We determined cell viability in the cells treated with ACR by use of CellTiter-Glo® assay. As shown in Figure 1, HL-60 cells were significantly more sensitive to 0.2 μM and 0.5 μM

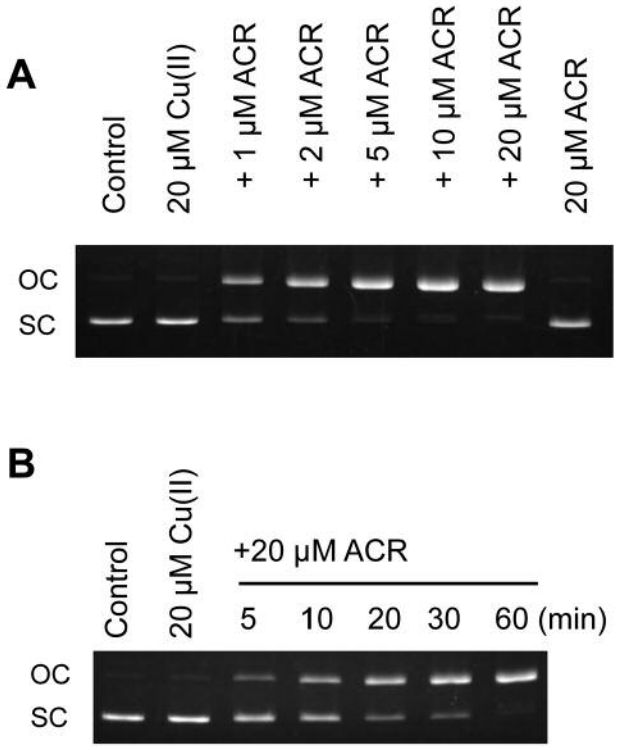

Figure 3. *Analysis of aclarubicin (ACR)-induced DNA damage in the presence of Cu(II). A: Plasmid pBR322 DNA was treated with the indicated concentrations of ACR in the presence of 20 μM $CuCl_2$ for 1 h. B: Plasmid pBR322 DNA was treated with 20 μM ACR in the presence of 20 μM $CuCl_2$ for the indicated times. The supercoiled (SC) and open circular (OC) forms of DNA are indicated.*

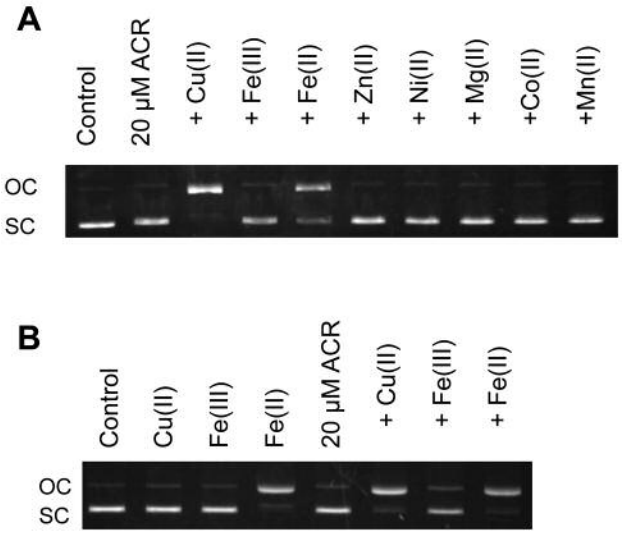

Figure 4. *Analysis of aclarubicin (ACR)-induced DNA damage in the presence of metals in a cell-free system. A: Plasmid pBR322 DNA was treated with 20 μM ACR in the presence of 20 μM a metal ($CuCl_2$, $FeCl_3$, $FeSO_4(NH_4)_2SO_4$, $ZnSO_4$, $NiSO_4$, $MgCl_2$, $CoCl_2$ or $MnCl_2$) 1 h. B: Plasmid pBR322 DNA was treated with 20 μM metal and 20 μM ACR for 1 h. The supercoiled (SC) and open circular (OC) forms of DNA are indicated.*

ACR than were HP100 cells after 6-h and 24-h incubation. The cytotoxicity of 24-h ACR treatment was higher than that of 6-h ACR treatment.

DNA ladder assay in HL-60 and HP100 cells treated with ACR. After treatment with ACR, DNA ladder formation, which reflects apoptotic events, was analyzed using conventional electrophoresis. In HL-60 cells, ACR-induced DNA ladder formation was detected after 6-h incubation with 0.2 and 0.5 μM, while it was only detected at 0.5 μM in HP100 cells (Figure 2A).

Caspase-3/7 activity in HL-60 and HP100 cells after ACR treatment. ACR-induced apoptosis was assessed by caspase-3/7 activity. The caspase-3/7 activity after 6-h ACR treatment was remarkably increased at 0.2 and 0.5 μM in HL-60 cells (0.2 μM, $p<0.01$; 0.5 μM, $p<0.001$), and at 0.5 μM in HP100 cells ($p<0.001$). Caspase-3/7 in HL-60 cells had significant higher activity than that in HP100 cells at 0.2 and 0.5 μM (Figure 2B) (0.2 μM, $p<0.001$; 0.5 μM, $p<0.05$). These events were in good agreement with DNA ladder formation induced by ACR.

ACR-induced DNA damage in the presence of Cu(II). Figure 3 shows agarose gel electrophoretic DNA cleavage patterns of plasmid DNA pBR322 after ACR treatment. The intensity of DNA damage increased depending on the ACR concentration in the presence of Cu(II) (Figure 3A). ACR induced DNA damage at 1 μM and clear strong DNA damage above 2 μM in the presence of Cu(II). ACR or Cu(II) did not induce DNA damage alone. The intensity of ACR-induced DNA damage also increased dependent on incubation time in the presence of Cu(II). DNA damage was induced by ACR at 5 min in the presence of Cu(II) (Figure 3B). On the other hand, DNA damage was not caused by ACR in the presence of Fe(III), Zn(II), Ni(II), Mg(II), Co(II) or Mn(II) (Figure 4A). Moreover, since Fe(II) alone induced DNA damage, it is suggested that ACR itself may not cause DNA damage in the presence of Fe(II) (Figure 4B).

Effects of ROS scavengers and bathocuproine on ACR-induced DNA damage in the presence of Cu(II). The effects of ROS scavengers and bathocuproine on ACR-induced DNA damage in the presence of Cu(II) in the cell-free system using plasmid DNA pBR322 are shown in Figure 5. Little or no inhibition of DNA damage induced by ACR was

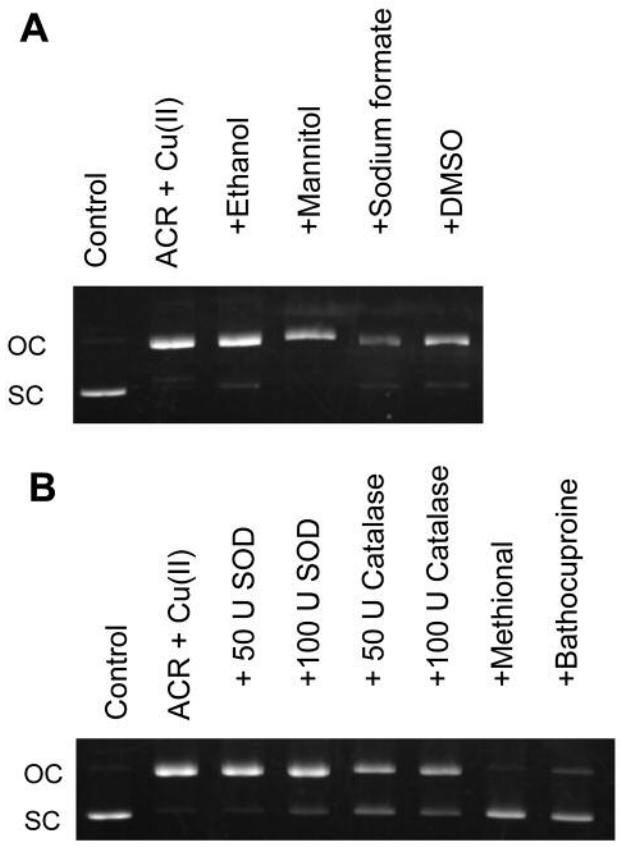

Figure 5. *Inhibition by scavengers of reactive oxygen species (ROS) and bathocuproine, a Cu(I)-chelating agent, of aclarubicin (ACR)-induced DNA cleavage in the presence of Cu(II). A: Plasmid pBR322 DNA was treated with 20 μM ACR in the presence of Cu(II) (20 μM) for 1 h with and without 1.7 M (10%) ethanol, 0.1 M mannitol, 0.1 M sodium formate, 0.7 M (10%) dimethyl sulfoxide (DMSO), 50 or 100 units of superoxide dismutase (SOD), 50 or 100 units of catalase, 0.1 M methional, or 50 μM bathocuproine was added. The supercoiled (SC) and open circular (OC) forms of DNA are indicated.*

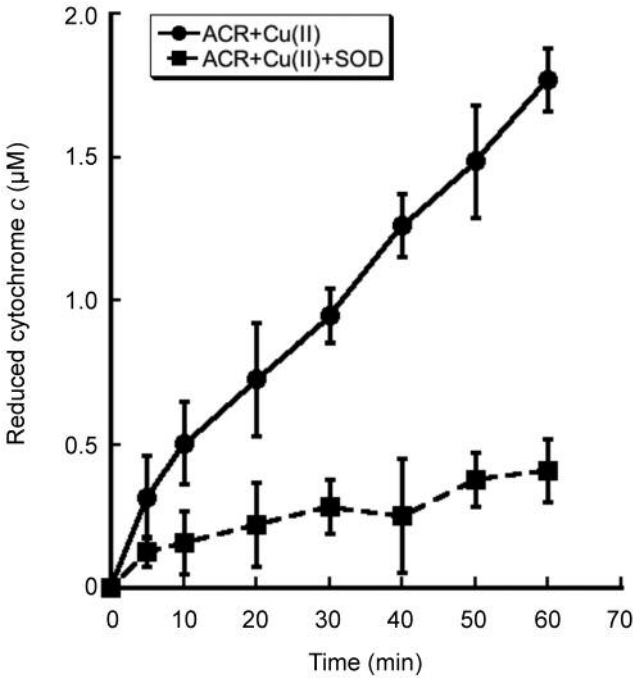

Figure 6. *Temporal pattern of the production of reduced cytochrome c with aclarubicin (ACR) in the presence of Cu(II). The reaction solution contained 100 μM cytochrome c, 20 μM ACR and 20 μM Cu(II). Absorption at 550 nm was measured at 37°C with a spectrophotometer. The actual amount of reduced cytochrome c was calculated by subtracting absorbance with 100 U/ml superoxide dismutase (SOD) from that without SOD at 550 nm (ε=21.1×10^3 M^{-1} cm^{-1}). The data are presented as means±SD (n=3).*

found after incubation with typical •OH scavengers, ethanol, mannitol, sodium formate and DMSO (Figure 5A). SOD and catalase inhibited DNA damage induced by ACR. Methional and bathocuproine completely inhibited DNA damage induced by ACR (Figure 5B).

Detection of $O_2^{\bullet-}$ derived from ACR in the presence of Cu(II) in a cell-free system. Figure 6 shows the production of reduced cytochrome *c* as a result of ACR in the presence Cu(II). The presence of ACR and Cu(II) led to a time-dependent increase in reduced cytochrome *c*. The quantity of reduced cytochrome *c* decreased with the addition of SOD, reflecting the production of $O_2^{\bullet-}$. From these results, the quantity of $O_2^{\bullet-}$ produced by 20 μM ACR was about 1.4 μM in the presence of 20 μM Cu(II). The inhibition of cytochrome *c* reduction by SOD was only partial, it suggests that there are $O_2^{\bullet-}$-independent mechanisms of reduction of cytochrome *c*, possibly mediated by Cu(I) (20, 23).

Determination of intracellular Cu(I) in HL-60 cells treated with ACR. Figure 7 shows intracellular Cu(I) detection induced by ACR in HL-60 cells. We used CopperGREEN™, a green fluorescent probe for detection of Cu(I) ions specifically, in order to determine intracellular Cu(I) in cultured cells (22). The results showed that ACR treatment coincided with an increase in Cu(I)-positive cells in a dose-dependent manner.

Discussion

In this study, we showed ACR induced apoptosis of both HL-60 cells and HP100 cells, the H_2O_2-resistant clone of HL-60. ACR-induced cytotoxicity, DNA ladder formation and caspase-3/7 activity of HP100 cells were suppressed, in comparison with that of HL-60 cells. HP100 cells have approximately 340-fold higher resistance to H_2O_2 than HL-60 cells (14). Therefore, these observations can be explained

by the mediation of H_2O_2 production in the apoptotic mechanism induced ACR. Our previous reports have shown that doxorubicin and pirarubicin induce oxidative DNA damage by H_2O_2 production, followed by mitochondrial dysfunction and subsequent activation of caspase-3/7, resulting in apoptosis (16, 24). Therefore, these observations show the possibility that oxidative DNA damage by H_2O_2 production induces apoptosis.

In order to verify the mechanism of DNA damage, we demonstrated that ACR induced oxidative DNA damage of plasmid DNA in the presence of Cu(II) in a cell-free system. DNA damage was inhibited by SOD and catalase, suggesting the involvement of $O_2^{\bullet-}$ and H_2O_2. Bathocuproine entirely inhibited DNA damage, since bathocuproine prevents H_2O_2-activation by chelating Cu(I) (25, 26). This suggests that Cu(I) is involved in DNA damage. As typical •OH scavengers (ethanol, mannitol, sodium formate and DMSO) did not prevent DNA damage, it is suggested that free •OH is not involved in DNA damage induced by ACR. Methional completely inhibited DNA damage. Methional inhibits not only •OH but also other radicals, for example, metal–oxygen complexes (27). Hence, Cu(II)-mediated DNA damage appears to be due to ROS such as Cu(I)OOH. Moreover, we demonstrated that ACR generated $O_2^{\bullet-}$ in the presence of Cu(II), suggesting that ACR and Cu(II) produced Cu(I), which reacted with O_2 to produce $O_2^{\bullet-}$ and subsequently H_2O_2. In addition, we revealed that ACR treatment generated intracellular Cu(I) using a fluorescent probe that specifically detects Cu(I) in HL-60 cells.

We previously demonstrated that doxorubicin and pirarubicin induced oxidative DNA damage in the presence of Cu(II) through oxidation of its *p*-hydroquinone moiety by copper ion (20, 23). ACR has an anthraquinone moiety similar to doxorubicin and pirarubicin. Therefore, it appears that ACR induces oxidative DNA damage in the presence of Cu(II) in a similar way to that of doxorubicin and pirarubicin. We propose the mechanism of ACR-induced oxidative DNA damage to be as follows: ACR undergoes Cu(II)-mediated one-electron oxidation at the OH group on the anthraquinone aromatic moiety to produce Cu(I) and the semiquinone radical. Cu(I) undergoes $O_2^{\bullet-}$ production from O_2, subsequently generating H_2O_2. DNA binding to produce Cu(I) interacts with H_2O_2, resulting in the formation of DNA–copper-hydroperoxo complex [DNA-Cu(I)OOH] (Figure 8). Although typical •OH scavengers did not prevent DNA damage, •OH may be involved in DNA damage mediated by the formation of DNA–Cu(I)OOH, which can release •OH in the proximity of DNA. •OH readily attacks an adjacent component of DNA, before it is inhibited by •OH scavengers (20, 23). Moreover, we demonstrated that ACR treatment generated intracellular Cu(I) in HL-60 cells, confirming that Cu(I) has important roles in ACR-induced DNA damage and apoptosis.

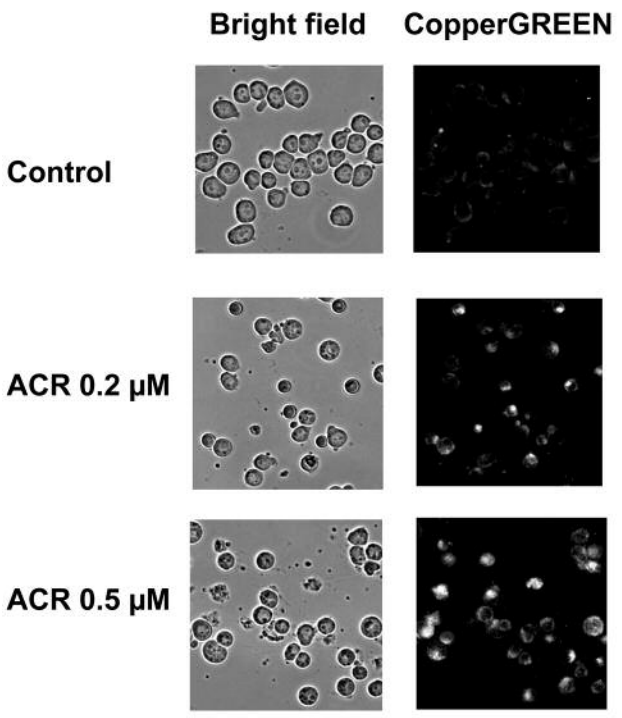

Figure 7. *Determination of intracellular Cu(I) generation induced by aclarubicin (ACR) in HL-60 cells. HL-60 cells (1×10^6 cells) were treated with ACR for 3 h in the presence of 5 μM CopperGREEN™, a fluorescent probe used to detect Cu(I) ion. Cells were washed twice with phosphate-buffered saline (PBS). After resuspension in PBS, cells were analyzed by fluorescence microscopy.*

Furthermore, it is reported that 40 μM of copper exist in the nucleus of the normal mouse hepatocytes (28, 29). DNA has greater affinity for copper ions than for other essential metal ions (29, 30). These findings suggest that ACR with intracellular copper may induce oxidative DNA damage in cells. Our and other groups reported that anticancer agents (doxorubicin, pirarubicin, hydroxyurea, procarbazine, cyclophosphamide, dacarbazine, 6-mercaptopurine, methotrexate and etoposide) in the presence of copper-induced oxidative DNA damage in a cell-free system (20, 23, 31-37). Previous reports described that anthracyclines induced ROS generation and oxidative DNA damage in the presence of iron (38, 39), whereas we demonstrated that H_2O_2 production and copper also have important roles in DNA-damaging and apoptotic activity of anthracyclines. Therefore, oxidative DNA damage, mediated by H_2O_2 production and copper, followed by apoptosis may be an important general anticancer mechanism for anthracyclines.

Conflicts of Interest

The Authors have no conflicts of interest to declare.

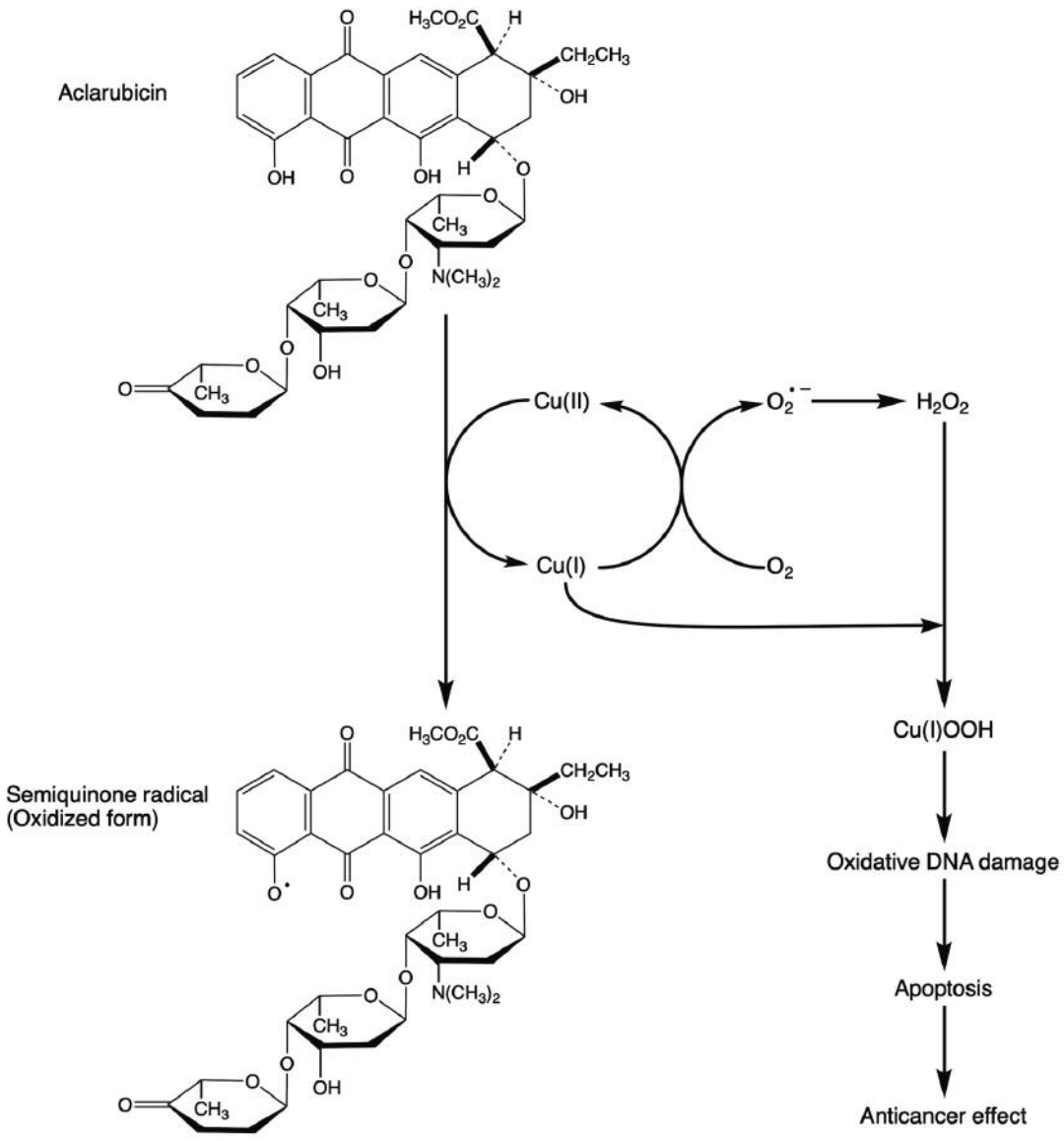

Figure 8. *Probable mechanisms for oxidative DNA damage and apoptosis induced by aclarubicin in the presence of Cu(II).*

Authors' Contributions

H.M., Y. Hayashi, M.H. and Y. Ichimaru contributed to the experimental work; all Authors participated in data analysis; H.M. and S.K. conceived and coordinated the study; H.M., Y. Hiraku and S.K. drafted the article. All Authors gave final approval for publication.

Acknowledgements

This work was supported by JSPS KAKENHI Grant Number 25460229 and 16K08420.

References

1 Wellstein A: Section VIII. Pharmacotherapy of Neoplastic Diseases. In: Brunton LL, Hilal-Dandan R and Knollmann BC (eds.): Goodman and Gilman's: The Pharmacological Basis of Therapeutics, 13th Edition. McGraw Hill. pp. 1159-1248, 2018.

2 Oki T, Matsuzawa Y, Yoshimoto A, Numata K, Kitamura I, Hori S, Takamatsu A, Umezawa H, Ishizuka M, Naganawa H, Suda H, Hamada M and Takeuchi T: New antitumor antibiotics, aclacinomycins A and B. J Antibiot *28*: 830-834, 1975. PMID: 1184473. DOI: 10.7164/antibiotics.28.830

3 Hori S, Shirai M, Hirano S, Oki T, Inui T, Tsukagoshi S, Ishizuka M, Takeuchi T and Umezawa H: Antitumor activity of new anthracycline antibiotics, aclacinomycin-A and its analogs, and their toxicity. Gan *68*: 685-690, 1977. PMID: 579346.

4 Wakabayashi T, Oki T, Tone H, Hirano S and Omori K: A comparative electron microscopic study of aclacinomycin and adriamycin cardiotoxicities in rabbits and hamsters. J Electron Microsc *29*: 106-118, 1980. PMID: 6933206.

5 Wei G, Ni W, Chiao JW, Cai Z, Huang H and Liu D: A meta-analysis of CAG (cytarabine, aclarubicin, G-CSF) regimen for the treatment of 1029 patients with acute myeloid leukemia and myelodysplastic syndrome. J Hematol Oncol *4*: 46, 2011. PMID: 22082134. DOI: 10.1186/1756-8722-4-46

6 Fukushima T, Kawabata H, Sawaki T, Satoh T, Nakamura T, Iwao H, Nakajima A, Sakai T, Miki M, Fujita Y, Tanaka M, Kawanami T, Masaki Y, Okazaki T and Umehara H: Low-dose cytarabine plus aclarubicin for patients with previously untreated acute myeloid leukemia or high-risk myelodysplastic syndrome ineligible for standard-dose cytarabine plus anthracycline. Anticancer Res *32*: 1347-1353, 2012. PMID: 22493369.

7 Minakata D, Fujiwara S, Ito S, Mashima K, Umino K, Nakano H, Kawasaki Y, Sugimoto M, Yamasaki R, Yamamoto C, Ashizawa M, Hatano K, Okazuka K, Sato K, Oh I, Ohmine K, Suzuki T, Muroi K and Kanda Y: A low-dose cytarabine, aclarubicin and granulocyte colony-stimulating factor priming regimen *versus* a daunorubicin plus cytarabine regimen as induction therapy for older patients with acute myeloid leukemia: A propensity score analysis. Leuk Res *42*: 82-87, 2016. PMID: 26790727. DOI: 10.1016/j.leukres.2015.12.013

8 Larsen AK, Escargueil AE and Skladanowski A: Catalytic topoisomerase II inhibitors in cancer therapy. Pharmacol Ther *99*: 167-181, 2003. PMID: 12888111. DOI: 10.1016/S0163-7258(03)00058-5

9 Misumi M, Yamaki H, Akiyama T and Tanaka N: Mechanism of action of aclacinomycin A II. The interaction with DNA and with tubulin. J Antibiot *32*: 48-52, 1979. PMID: 761992. DOI: 10.7164/antibiotics.32.48

10 Ando S, Kamiya K, Yoshimura T, Tsutani H, Ueda T, Uchida M, Nakamura T and Uchino H: DNA-binding characteristics of aclarubicin as compared with daunorubicin and doxorubicin. Anticancer Res *8*: 409-415, 1988. PMID: 3164610.

11 Rogalska A, Koceva-Chyła A and Jóźwiak Z: Aclarubicin-induced ROS generation and collapse of mitochondrial membrane potential in human cancer cell lines. Chem Biol Interact *176*: 58-70, 2008. PMID: 18692031. DOI: 10.1016/j.cbi.2008.07.002

12 Kania K, Zych A and Jóźwiak Z: Involvement of reactive oxygen species in aclarubicin-induced death of human trisomic and diabetic fibroblasts. Toxicol In Vitro *21*: 1010-1019, 2007. PMID: 17459657. DOI: 10.1016/j.tiv.2007.02.013

13 Rogalska A, Szwed M and Jóźwiak Z: Aclarubicin-induced apoptosis and necrosis in cells derived from human solid tumours. Mutat Res *700*: 1-10, 2010. PMID: 20399885. DOI: 10.1016/j.mrgentox.2010.04.013

14 Kasugai I and Yamada M: Adaptation of human leukemia HL-60 cells to hydrogen peroxide as oxidative stress. Leuk Res *13*: 757-762, 1989. PMID: 2796382. DOI: 10.1016/0145-2126(89)90088-X

15 Kasugai I and Yamada M: High production of catalase in hydrogen peroxide-resistant human leukemia HL-60 cell lines. Leuk Res *16*: 173-179, 1992. PMID: 1312186. DOI: 10.1016/0145-2126(92)90129-U

16 Mizutani H, Hotta S, Nishimoto A, Ikemura K, Miyazawa D, Ikeda Y, Maeda T, Yoshikawa M, Hiraku Y and Kawanishi S: Pirarubicin, an anthracycline anticancer agent, induces apoptosis through generation of hydrogen peroxide. Anticancer Res *37*: 6063-6069, 2017. PMID: 29061786. DOI: 10.21873/anticanres.12054

17 Hiraku Y and Kawanishi S: DNA damage and apoptosis induced by benzene metabolites. Cancer Res *56*: 5172-5178, 1996. PMID: 8912853.

18 Mizutani H, Tada-Oikawa S, Hiraku Y, Oikawa S, Kojima M and Kawanishi S: Mechanism of apoptosis induced by a new topoisomerase inhibitor through the generation of hydrogen peroxide. J Biol Chem *277*: 30684-30689, 2002. PMID: 12068015. DOI: 10.1074/jbc.M204353200

19 Ohnishi S, Mizutani H and Kawanishi S: The enhancement of oxidative DNA damage by anti-diabetic metformin, buformin, and phenformin, *via* nitrogen-centered radicals. Free Radic Res *50*: 929-937, 2016. PMID: 27328723. DOI: 10.1080/10715762.2016.1204651

20 Mizutani H, Nishimoto A, Hotta S, Ikemura K, Imai M, Miyazawa D, Ohta K, Ikeda Y, Maeda T, Yoshikawa M, Hiraku Y and Kawanishi S: Oxidative DNA damage induced by pirarubicin, an anthracycline anticancer agent, in the presence of copper(II). Anticancer Res *38*: 2643-2648, 2018. PMID: 29715084. DOI: 10.21873/anticanres.12506

21 Mizutani H, Hiraku Y, Tada-Oikawa S, Murata M, Ikemura K, Iwamoto T, Kagawa Y, Okuda M and Kawanishi S: Romidepsin (FK228), a potent histone deacetylase inhibitor, induces apoptosis through the generation of hydrogen peroxide. Cancer Sci *101*: 2214-2219, 2010. PMID: 20624163. DOI: 10.1111/j.1349-7006.2010.01645.x

22 Taki M, Iyoshi S, Ojida A, Hamachi I and Yamamoto Y: Development of highly sensitive fluorescent probes for detection of intracellular copper(I) in living systems. J Am Chem Soc *132*: 5938-5939, 2010. PMID: 20377254. DOI: 10.1021/ja100714p

23 Mizutani H, Oikawa S, Hiraku Y, Murata M, Kojima M and Kawanishi S: Distinct mechanisms of site-specific oxidative DNA damage by doxorubicin in the presence of copper(II) and NADPH-cytochrome P450 reductase. Cancer Sci *94*: 686-691, 2003. PMID: 12901793.

24 Mizutani H, Tada-Oikawa S, Hiraku Y, Kojima M and Kawanishi S: Mechanism of apoptosis induced by doxorubicin through the generation of hydrogen peroxide. Life Sci *76*: 1439-1453, 2005. PMID: 15680309. DOI: 10.1016/j.lfs.2004.05.040

25 Jewett SL, Rocklin AM, Ghanevati M, Abel JM and Marach JA: A new look at a time-worn system: oxidation of CuZn-SOD by H_2O_2. Free Radic Biol Med *26*: 905-918, 1999. PMID: 10232834.

26 Burkitt MJ: A critical overview of the chemistry of copper-dependent low density lipoprotein oxidation: roles of lipid hydroperoxides, alpha-tocopherol, thiols, and ceruloplasmin. Arch Biochem Biophys *394*: 117-135, 2001. PMID: 11566034. DOI: 10.1006/abbi.2001.2509

27 Pryor WA and Tang RH: Ethylene formation from methional. Biochem Biophys Res Commun *81*: 498-503, 1978. PMID: 666768.

28 Ralle M, Huster D, Vogt S, Schirrmeister W, Burkhead JL, Capps TR, Gray L, Lai B, Maryon E and Lutsenko S: Wilson disease at a single-cell level: Intracellular copper trafficking activates compartment-specific responses in hepatocytes. J Biol Chem *285*: 30875-30883, 2010. PMID: 20647314. DOI: 10.1074/jbc.M110.114447

29 Linder MC: The relationship of copper to DNA damage and damage prevention in humans. Mutat Res *733*: 83-91, 2012. PMID: 23463874.

30 Burkitt MJ: Copper--DNA adducts. Methods Enzymol *234*: 66-79, 1994. PMID: 7808340.

31 Sakano K, Oikawa S, Hasegawa K and Kawanishi S: Hydroxyurea induces site-specific DNA damage *via* formation of hydrogen peroxide and nitric oxide. Jpn J Cancer Res *92*: 1166-1174, 2001. PMID: 11714440.

32 Ogawa K, Hiraku Y, Oikawa S, Murata M, Sugimura Y, Kawamura J and Kawanishi S: Molecular mechanisms of DNA damage induced by procarbazine in the presence of Cu(II). Mutat Res *539*: 145-155, 2003. PMID: 12948823.

33 Murata M, Suzuki T, Midorikawa K, Oikawa S and Kawanishi S: Oxidative DNA damage induced by a hydroperoxide derivative of cyclophosphamide. Free Radic Biol Med *37*: 793-802, 2004. PMID: 15304255. DOI: 10.1016/j.freerad biomed.2004.05.009

34 Iwamoto T, Hiraku Y, Okuda M and Kawanishi S: Mechanism of UVA-dependent DNA damage induced by an antitumor drug dacarbazine in relation to its photogenotoxicity. Pharm Res *25*: 598-604, 2008. PMID: 17710513. DOI: 10.1007/s11095-007-9413-2

35 Rehman SU, Zubair H, Sarwar T, Husain MA, Ishqi HM, Nehar S and Tabish M: Redox cycling of Cu(II) by 6-mercaptopurine leads to ROS generation and DNA breakage: Possible mechanism of anticancer activity. Tumour Biol *36*: 1237-1244, 2015. PMID: 25344215. DOI: 10.1007/s13277-014-2743-x

36 Nagaj J, Kołkowska P, Bykowska A, Komarnicka UK, Kyzioł A and Jeżowska-Bojczuk M: Interaction of methotrexate, an anticancer agent, with copper(II) ions: coordination pattern, DNA-cleaving properties and cytotoxic studies. Med Chem Res *24*: 115-123, 2015. PMID: 25589824.

37 Sinha BK, Antholine WM, Kalyanaraman B and Eliot HM: Copper ion-dependent oxy-radical mediated DNA damage from dihydroxy derivative of etoposide. Biochim Biophys Acta *1096*: 81-83, 1990. PMID: 2176549.

38 Stěrba M, Popelová O, Vávrová A, Jirkovský E, Kovaříková P, Geršl V and Simůnek T: Oxidative stress, redox signaling, and metal chelation in anthracycline cardiotoxicity and pharmacological cardioprotection. Antioxid Redox Signal *18*: 899-929, 2013. PMID: 22794198. DOI: 10.1089/ars.2012.4795

39 Gammella E, Maccarinelli F, Buratti P, Recalcati S and Cairo G: The role of iron in anthracycline cardiotoxicity. Front Pharmacol *5*: 25, 2014. PMID: 24616701. DOI: 10.3389/fphar.2014.00025

Received April 27, 2019
Revised June 4, 2019
Accepted June 7, 2019